

# Search for Lorentz-violation through sidereal effect at NO $\nu$ A Experiment

Shashank Mishra,<sup>1,2</sup> Saurabh Shukla,<sup>1,2,\*</sup> Lakhwinder Singh,<sup>1,†</sup> and Venktesh Singh<sup>1</sup>

<sup>1</sup>*Department of Physics, Central University of South Bihar, Gaya 824236, India*

<sup>2</sup>*Department of Physics, Institute of Science, Banaras Hindu University, Varanasi 221005, India.*

(Dated: September 6, 2023)

Long-baseline neutrino oscillation experiments offer a unique laboratory to test the fundamental Lorentz symmetry, which is heart of both the standard model of particle and general relativity theory. Deviations from the standard neutrino oscillation or the sidereal modulation in neutrino events will smoking-gun experimental signature of Lorentz and CPT violation. In this study, we investigate the impact of the sidereal effect on standard neutrino oscillation measurements within the context of the NO $\nu$ A experiment. Additionally, we assess the sensitivity of the NO $\nu$ A experiment to detect Lorentz-violating interactions, taking into account the sidereal effect. Furthermore, we highlight potential of the NO $\nu$ A experiment to set the new constraints on anisotropic Lorentz-violating parameters.

PACS numbers: 11.30.Cp, 14.60.Pq, 14.60.St

Keywords: Neutrino mass and mixing, Lorentz Invariance Violation, NO $\nu$ A

## I. INTRODUCTION:

Lorentz symmetry is a key assumption in our present understanding of high-energy processes and ensures the all inertial observers perceive the physical phenomenon identically. This symmetry, however, raises the question of testability in ultra-high energy theories at the Planck scale physics such as string theory [1, 2], loop quantum gravity [3], brane-worlds scenarios [4]. These theories unify the gravity and gauge fields of the Standard Model (SM) of particle physics by allowing small perturbation of Lorentz symmetry breaking, so-called Lorentz Invariance Violation (LIV) [5]. The Standard Model Extension (SME) serves as a effective theory of above mentioned ultra-high energy theories. The SME incorporates complete range of particles and interactions of SM as well as additional all possible Lorentz violation operators, therefore, provides a feasible framework for LIV searches in a variety of scenarios like gravity, charged leptons, photons, nucleons, and neutrinos [6–8].

The discovery of “finite neutrino masses and mixings” with various neutrino sources is the first evidence of the existence of physics beyond the SM [9–11]. Over the last two decades, there is a tremendous development in neutrino experiments, allowing us to enter the era of precision measurement. LIV parameters are classified as isotropic and anisotropic. In experiments where both the neutrino source and detector are located on the Earth, the observed sidereal modulation in neutrino events provides the smoking-gun signature of a non-zero anisotropic LIV parameters. Several neutrino experiments are performed to observe the LIV including MINOS-FD [12], MINOS-ND [13, 14], IceCube [15], LSND [16], Super-K [17], T2K [18], DayaBay [19], MiniBooNE [20], Double Chooz [21], etc. Previous experimental searches for

LIV using the sidereal effect have primarily concentrated on short baseline neutrino oscillation experiments or exclusively targeted the time-independent isotropic components [22]. The aim of this work is to expand and improve the sensitivity of LIV parameters in the non-isotropic time dependence case. We study the impact for sidereal time to the LIV parameters in the context of NO $\nu$ A experiment which is a long baseline neutrino experiment [23]. We simulate the neutrino events in appearance and disappearance channel considering the effective Hamiltonian which contain LIV and CPT perturbative terms.

This article is structured as follows. The general formulation of effective Hamiltonian is discussed in Sec. II. The effective Hamiltonian is also restructured to study sidereal effect. Our approach to simulation, adopted experimental design and standard oscillation parameters are outlined in Sec. III. In Sec. IV, we present sensitivity of NO $\nu$ A experiment to determine the CP violating phase ( $\delta_{cp}$ ) and  $\theta_{23}$  in the presence of LIV parameters. Additionally, we also present upper limits for all 12 LIV parameters under sidereal analysis and compare with existing upper limits from literature and conclude in Sec. V.

## II. FORMALISM

In a lepton sector, the general form of the Lorentz violating part of the SME Lagrangian can be divided into CPT-even and CPT-odd terms [6]:

$$\begin{aligned} \mathcal{L}_{\text{LIV}}^{\text{CPT-even}} = & -\frac{1}{2}(H_L)_{\mu\nu AB}\bar{l}_A\sigma^{\mu\nu}l_B \\ & + -\frac{1}{2}i(c_L)_{\mu\nu AB}\bar{l}_A\gamma^\mu \leftrightarrow D^\nu l_B \\ & + -\frac{1}{2}i(d_L)_{\mu\nu AB}\bar{l}_A\gamma_5\gamma^\mu \leftrightarrow D^\nu l_B, \end{aligned} \quad (1)$$

\* saurabhps099@gmail.com

† lakhwinder@cusb.ac.in

where  $(H_L)_{\mu\nu AB}$  are antisymmetric coupling coefficients with dimensions of mass.  $(c_L)_{\mu\nu AB}$  and  $(d_L)_{\mu\nu AB}$  are symmetric and antisymmetric hermitian dimensionless couplings coefficients, respectively.

$$\mathcal{L}_{LIV}^{CPT-odd} = -(a_L)_{\mu AB} \bar{l}_A \gamma^\mu l_B - (b_L)_{\mu AB} \bar{l}_A \gamma_5 \gamma^\mu l_B, \quad (2)$$

where  $(a_L)_{\mu AB}$  and  $(b_L)_{\mu AB}$  are hermitian CPT-breaking LIV coupling coefficients with dimension of mass.

In the Hamiltonian picture, the effective Hamiltonian  $(\mathcal{H}_{eff})_{\alpha\beta}$  of neutrinos with small LIV and CPT violating perturbation is generally written as [24]

$$(\mathcal{H}_{eff})_{\alpha\beta} = (\mathcal{H}_o)_{\alpha\beta} + (\mathcal{H}_{LIV})_{\alpha\beta}, \quad (3)$$

where  $(\mathcal{H}_o)_{\alpha\beta}$  is a conventional standard neutrino Hamiltonian, describes the Lorentz-invariant neutrino oscillation and  $(\mathcal{H}_{LIV})_{\alpha\beta}$  is a perturbative hamiltonian including LIV contributions. The Indices  $\alpha$  and  $\beta$  represent the three neutrino flavors. In general  $(\mathcal{H}_{eff})_{\alpha\beta}$  is a  $6 \times 6$  matrix which can be represented as:

$$(\mathcal{H}_{eff}) = \begin{pmatrix} (\mathcal{H}_o)_{\nu\nu} & 0 \\ 0 & (\mathcal{H}_o)_{\bar{\nu}\bar{\nu}} \end{pmatrix} + \begin{pmatrix} (\mathcal{H}_{liv})_{\nu\nu} & (\mathcal{H}_{liv})_{\nu\bar{\nu}} \\ (\mathcal{H}_{liv})_{\bar{\nu}\nu} & (\mathcal{H}_{liv})_{\bar{\nu}\bar{\nu}} \end{pmatrix}, \quad (4)$$

where  $(\mathcal{H}_o)_{\nu\nu}((\mathcal{H}_o)_{\bar{\nu}\bar{\nu}})$  is standard neutrino(anti-neutrino) Hamiltonian term which is responsible for standard neutrino(anti-neutrino) oscillations. Diagonal terms  $(\mathcal{H}_{liv})_{\nu\nu}$  and  $(\mathcal{H}_{liv})_{\bar{\nu}\bar{\nu}}$  are contributing for neutrino-neutrino oscillation and antineutrino-antineutrino oscillation, respectively. Off-diagonal components, namely  $(\mathcal{H}_{liv})_{\nu\bar{\nu}}$  and  $(\mathcal{H}_{liv})_{\bar{\nu}\nu}$  are govern neutrino-antineutrino oscillations and vice versa.

The standard neutrino(anti-neutrino) oscillation is parameterized by two mass square differences  $\Delta m_{21}^2$ ,  $\Delta m_{31}^2$ , three mixing angles  $\theta_{12}$ ,  $\theta_{23}$ ,  $\theta_{13}$  and a phase  $\delta_{cp}$ . In this

study, we solely conform to neutrino-neutrino oscillation and corresponding Hamiltonian can be explicitly written as

$$(\mathcal{H}_o)_{\nu\nu} = \frac{1}{E} \left[ U \begin{pmatrix} 0 & 0 & 0 \\ 0 & \Delta m_{21}^2 & 0 \\ 0 & 0 & \Delta m_{31}^2 \end{pmatrix} U^\dagger + V_{matter} \right], \quad (5)$$

where the PMNS matrix  $U$  is parameterized as Ref [25] and  $V_{matter}$  is matter potential includes the matter effect. In the minimal SME, the interactions and neutrino propagation are both governed by the following leading-order effective hamiltonian [26]

$$((\mathcal{H}_{liv})_{\nu\nu})_{\alpha\beta} = |\vec{p}| \delta_{\alpha\beta} + \frac{1}{|\vec{p}|} [(a)^\mu p_\mu - (c)^{\mu\nu} p_\mu p_\nu]_{\alpha\beta}, \quad (6)$$

where  $(a)^\mu$  and  $(c)^{\mu\nu}$  can be expressed as

$$(a)^\mu = \frac{1}{2}((a_L) + (b_L))^\mu, (c)^{\mu\nu} = \frac{1}{2}((c_L) + (d_L))^{\mu\nu}. \quad (7)$$

$(a)^\mu$  and  $(c)^{\mu\nu}$  are  $3 \times 3$  complex matrices represent LIV coefficients with mass dimension 1 and 0, respectively. The 4-momentum  $p_\mu = (|\vec{p}|, \vec{p})$  introduces the energy and momentum dependencies in the Hamiltonian. It implies that the mixing behavior of neutrino flavor would depend on the direction of neutrino propagation, which cause the rotational-symmetry violation. For the earth-based experiment, where the source and detector are fixed on the Earth's surface, the rotation of earth around its axis generates sidereal variation in oscillation probabilities can occur at multiples of the Earth's sidereal frequency  $\omega_\oplus \simeq 2\pi/(23 \text{ h } 56 \text{ min})$ . In order to compare the results from different experiments, it is convenient to adopt a common inertial frame. In the literature, measurements and sensitivities are conventionally expressed in terms of LIV coefficients defined in a Sun-centered celestial equatorial frame with coordinates (T,X,Y,Z). The effective Hamiltonian with sidereal time dependencies in the Sun-centered celestial equatorial frame can be expressed as :

$$\begin{aligned} (\mathcal{H}_{liv})_{\alpha\beta} = & (C)_{\alpha\beta} + R[a_{\alpha\beta}^X - 2E(c^{TX})_{\alpha\beta} + 2EN_z(c^{XZ})_{\alpha\beta}] \sin(\omega_\oplus T - \Phi_{orientation}) - \\ & R[a_{\alpha\beta}^Y - 2E(c^{TY})_{\alpha\beta} + 2EN_z(c^{YZ})_{\alpha\beta}] \cos(\omega_\oplus T - \Phi_{orientation}) + \\ & R^2[E \frac{1}{2}((c^{XX})_{\alpha\beta} - (c^{YY})_{\alpha\beta})] \cos(2(\omega_\oplus T + \Phi_{orientation})) + \\ & R^2[E(c^{XY})_{\alpha\beta}] \sin(2(\omega_\oplus T - \Phi_{orientation})), \end{aligned} \quad (8)$$

where  $T$  is the sidereal time, describes the earth's rotation w.r.t. a sidereal star in sun-centered frame. Amplitudes  $(C)_{\alpha\beta}$ ,  $\Phi_{orientation}$  and  $R$  can be expressed in the directional factors  $N^X$ ,  $N^Y$ ,  $N^Z$  in the following manner:

$$\Phi_{orientation} = \tan^{-1}(N^Y/N^X), \quad (9)$$

$$R = \sqrt{N_X^2 + N_Y^2}, \quad (10)$$

$$\begin{aligned} (C)_{\alpha\beta} = & (a)_{\alpha\beta}^T - N^Z (a)_{\alpha\beta}^Z + E[-\frac{1}{2}(3 - N^Z N^Z)(c)_{\alpha\beta}^{TT} \\ & + 2N^Z (c)_{\alpha\beta}^{TZ} + \frac{1}{2}(3 - N^Z N^Z)(c)_{\alpha\beta}^{ZZ}]. \end{aligned} \quad (11)$$

The directional factors ( $N^X$ ,  $N^Y$ ,  $N^Z$ ) are further expressed in terms of the angle between the beam and the vertically upward direction ( $\theta$ ) known as ‘‘Zenith’’ angle; the angle between the beam and the south measured towards the east ( $\phi$ ) known as ‘‘bearing’’ angle; and the colatitude of the detector ( $\chi$ ) [27].

$$\begin{aligned} N^X &= \cos \chi \sin \theta \cos \phi + \sin \chi \cos \theta, \\ N^Y &= \sin \theta \sin \phi, \\ N^Z &= -\sin \chi \sin \theta \cos \phi + \cos \chi \cos \theta, \end{aligned} \quad (12)$$

The LIV coefficients  $(a)_\alpha$  are solely governed by the baseline, while coefficients  $(c)_{\alpha\beta}$  are subject to control from both the baseline length and the energy of the neutrinos. The parameters  $(a)_{\alpha\beta}^T, (a)_{\alpha\beta}^Z, (c)_{\alpha\beta}^{TT}, (c)_{\alpha\beta}^{TZ}$  and  $(c)_{\alpha\beta}^{ZZ}$  belong  $(C)_{\alpha\beta}$  has no sidereal time dependency in the

perturbation, while the parameters  $(a)_{\alpha\beta}^X, (a)_{\alpha\beta}^Y, (c)_{\alpha\beta}^{TX}, (c)_{\alpha\beta}^{TY}, (c)_{\alpha\beta}^{XX}, (c)_{\alpha\beta}^{XY}, (c)_{\alpha\beta}^{XZ}, (c)_{\alpha\beta}^{YY}$  and  $(c)_{\alpha\beta}^{YZ}$  are responsible for sidereal modulation of perturbed hamiltonian terms. According to Eq. 8, a rotational transformation in the XY plane makes the parameters  $(a)_{\alpha\beta}^X$  and  $(a)_{\alpha\beta}^Y$  identical. The same is also true for pairs  $((c)_{\alpha\beta}^{TX}, (c)_{\alpha\beta}^{TY}), ((c)_{\alpha\beta}^{XX}, (c)_{\alpha\beta}^{YY})$  and  $((c)_{\alpha\beta}^{XZ}, (c)_{\alpha\beta}^{YZ})$ . Consequently, this work focuses on only 12 parameters  $((a)_{e\mu}^X, (a)_{e\tau}^X, (a)_{\mu\tau}^X, (c)_{e\mu}^{TX}, (c)_{e\tau}^{TX}, (c)_{\mu\tau}^{TX}, (c)_{e\mu}^{XX}, (c)_{e\tau}^{XX}, (c)_{\mu\tau}^{XX}, (c)_{e\mu}^{XZ}, (c)_{e\tau}^{XZ}, (c)_{\mu\tau}^{XZ})$ .

If the contribution of LIV perturbation in Eq. 3 is sufficiently small, the oscillation probabilities for both the appearance and disappearance channels can be expressed up to the leading order for the  $\mu e$  and  $\mu\mu$  channels, similarly as presented in Ref [34–41].

$$\begin{aligned} P_{\mu e}^{\text{LIV}} &\simeq x^2 f^2 + 2xyfg \cos(\Delta + \delta_{CP}) + y^2 g^2 + 4r_A |h_{e\mu}^{\text{LIV}}| \{xf[f s_{23}^2 \cos(\phi_{e\mu}^{\text{LIV}} + \delta_{CP}) + g c_{23}^2 \cos(\Delta + \delta_{CP} + \phi_{e\mu}^{\text{LIV}})] \\ &+ yg[g c_{23}^2 \cos \phi_{e\mu}^{\text{LIV}} + f s_{23}^2 \cos(\Delta - \phi_{e\mu}^{\text{LIV}})]\} + 4r_A |h_{e\tau}^{\text{LIV}}| s_{23} c_{23} \{xf[f \cos(\phi_{e\tau}^{\text{LIV}} + \delta_{CP}) - g \cos(\Delta + \delta_{CP} + \phi_{e\tau}^{\text{LIV}})] \\ &- yg[g \cos \phi_{e\tau}^{\text{LIV}} - f \cos(\Delta - \phi_{e\tau}^{\text{LIV}})]\} + 4r_A^2 g^2 c_{23}^2 |c_{23}| |h_{e\mu}^{\text{LIV}}| - s_{23} |h_{e\tau}^{\text{LIV}}|^2 + 4r_A^2 f^2 s_{23}^2 |s_{23}| |h_{e\mu}^{\text{LIV}}| + c_{23} |h_{e\tau}^{\text{LIV}}|^2 \\ &+ 8r_A^2 f g s_{23} c_{23} \{c_{23} \cos \Delta [s_{23} (|h_{e\mu}^{\text{LIV}}|^2 - |h_{e\tau}^{\text{LIV}}|^2) + 2c_{23} |h_{e\mu}^{\text{LIV}}| |h_{e\tau}^{\text{LIV}}| \cos(\phi_{e\mu}^{\text{LIV}} - \phi_{e\tau}^{\text{LIV}})] \\ &- |h_{e\mu}^{\text{LIV}}| |h_{e\tau}^{\text{LIV}}| \cos(\Delta - \phi_{e\mu}^{\text{LIV}} + \phi_{e\tau}^{\text{LIV}})\} + \mathcal{O}(s_{13}^2 a, s_{13} a^2, a^3), \end{aligned} \quad (13)$$

$$\begin{aligned} P_{\mu\mu}^{\text{LIV}} &\simeq 1 - \sin^2 2\theta_{23} \sin^2 \Delta - |h_{\mu\tau}^{\text{LIV}}| \cos \phi_{\mu\tau}^{\text{LIV}} \sin 2\theta_{23} \left[ (2r_A \Delta) \sin^2 2\theta_{23} \sin 2\Delta + 4 \cos^2 2\theta_{23} r_A \sin^2 \Delta \right] \\ &+ (|h_{\mu\mu}^{\text{LIV}}| - |h_{\tau\tau}^{\text{LIV}}|) \sin^2 2\theta_{23} \cos 2\theta_{23} \left[ (r_A \Delta) \sin 2\Delta - 2r_A \sin^2 \Delta \right], \end{aligned} \quad (14)$$

where

$$\begin{aligned} s_{ij} &= \sin \theta_{ij}, \quad c_{ij} = \cos \theta_{ij}, \quad x = 2s_{13}s_{23}, \quad y = 2rs_{12}c_{12}c_{23}, \quad r = |\Delta m_{21}^2 / \Delta m_{31}^2|, \quad \Delta = \frac{\Delta m_{31}^2 L}{4E}, \\ V_{CC} &= \sqrt{2} G_F N_e, \quad r_A = \frac{2E}{\Delta m_{31}^2}, \quad f = \frac{\sin[\Delta(1 - r_A(V_{CC} + h_{ee}^{\text{LIV}}))]}{1 - r_A(V_{CC} + h_{ee}^{\text{LIV}})}, \quad g = \frac{\sin[\Delta r_A(V_{CC} + h_{ee}^{\text{LIV}})]}{r_A(V_{CC} + h_{ee}^{\text{LIV}})}. \end{aligned} \quad (15)$$

The antineutrino probability  $P_{\bar{\mu}\bar{e}}^{\text{LIV}}$  ( $P_{\bar{\mu}\bar{\mu}}^{\text{LIV}}$ ) can be obtained from Eq. 13 (Eq. 14) by replacing  $V_{CC} \rightarrow -V_{CC}$ ,  $\delta_{CP} \rightarrow -\delta_{CP}$  and  $a_{\alpha\beta} \rightarrow -a_{\alpha\beta}^*$ . Similar expression for inverse hierarchy can be obtained by substituting  $\Delta m_{31}^2 \rightarrow -\Delta m_{31}^2$ , i.e.,  $\Delta \rightarrow -\Delta$  and  $r_A \rightarrow -r_A$ .

### III. NUMERICAL PROCEDURE OF SIMULATION

NuMI Off-Axis  $\nu_e$  Appearance Experiment (NO $\nu$ A), a long baseline experiment at Fermilab, examines neutrino oscillations using a high-intensity and high-purity beam of either muon neutrinos or muon antineutrinos. The experiment utilizes two identical detectors: a Far

Detector (FD) and a Near Detector (ND). The fiducial mass of FD is 14 kTon, and it is situated 810 KM away from the target and 14 mRad off axis [28]. As a fixed baseline experiment, NO $\nu$ A can observe the sidereal variation in the neutrino event rate in FD arising from the Earth’s rotation. In order to study the oscillation probabilities and event rate for NO $\nu$ A experiment, we adopted GLoBES [29] [30] software package with suitable modifications in *snu.c* plugin to include the sidereal effect. A exposure total of  $2.5 \times 10^{21}$  protons on target (POT) is utilized for the analysis of neutrinos, and an identical exposure is applied for antineutrinos. The POT is independent of sidereal time and remains constant throughout the time bin. For both the appearance and disappearance channels, the energy window is fixed from 1.0 GeV

to 5.0 GeV, with a peak value at 2.0 GeV.

Table I provides a summary of the standard oscillation parameters used in the simulation work. Since NO $\nu$ A is not sensitive for the mixing angle  $\theta_{12}$  and  $\theta_{13}$  [31]. These parameters are well-measured by other neutrino oscillation experiments, hence their values is fixed in simulation. The latest data of NO $\nu$ A experiment favor the normal neutrino mass hierarchy by  $1.9\sigma$  [23], therefore the normal mass ordering is also fixed throughout the simulation. Details on the beam orientation and FD of NO $\nu$ A experiment, which is employed for the simulation, are represented in Table II.

TABLE I. The standard oscillation parameters are used in this work. [32]

Parameter	True Value	Test Value
$\theta_{12}$	$33.48^\circ$	–
$\theta_{13}$	$8.5^\circ$	–
$\theta_{23}$	$45.0^\circ$	$(41.0^\circ, 52.0^\circ)$
$\delta_{cp}$	$195.0^\circ$	$(0^\circ, 360.0^\circ)$
$\Delta m_{21}^2$	$7.55 \times 10^{-5} eV^2$	–
$\Delta m_{31}^2$	$2.50 \times 10^{-3} eV^2$	–

TABLE II. NO $\nu$ A FD orientation details used in the simulation. [28]

Parameter	Value
$\chi$ co-latitude	$48.3793^\circ$
$\theta$ zenith angle	$84.26^\circ$
$\phi$ bearing	$204.616^\circ$

#### IV. RESULTS AND DISCUSSION

The standard neutrino oscillation probability spectrum without LIV parameters for appearance and disappearance channels with respect to energy and local sidereal time (LST) is depicted in top and bottom of the Fig. 1, respectively. All energies of neutrinos have a smooth probability-LST distribution throughout the whole sidereal time. However, there is a considerable distortion in the standard neutrino oscillation probability distribution when LIV parameters are taken into account as shown in Figs. 2 and 3.

In order to analysis the impact of LIV parameters on

the probability-LST distribution, a series of tests is designed with one LIV coefficient set to be very small value such as  $1 \times 10^{-23}$  and all other LIV coefficients set to zero. The first, second, third, and fourth panels (from left to right) of Figs. 2 and 3 illustrate the distortion in the standard neutrino oscillation probability distribution, when  $(a)^X$ ,  $(c)^{XX}$ ,  $(c)^{TX}$ , and  $(c)^{XZ}$  coefficients set to non-zero value, respectively. The top, middle, and bottom panels represent  $e\mu$ ,  $e\tau$ , and  $\mu\tau$  coefficients, respectively.

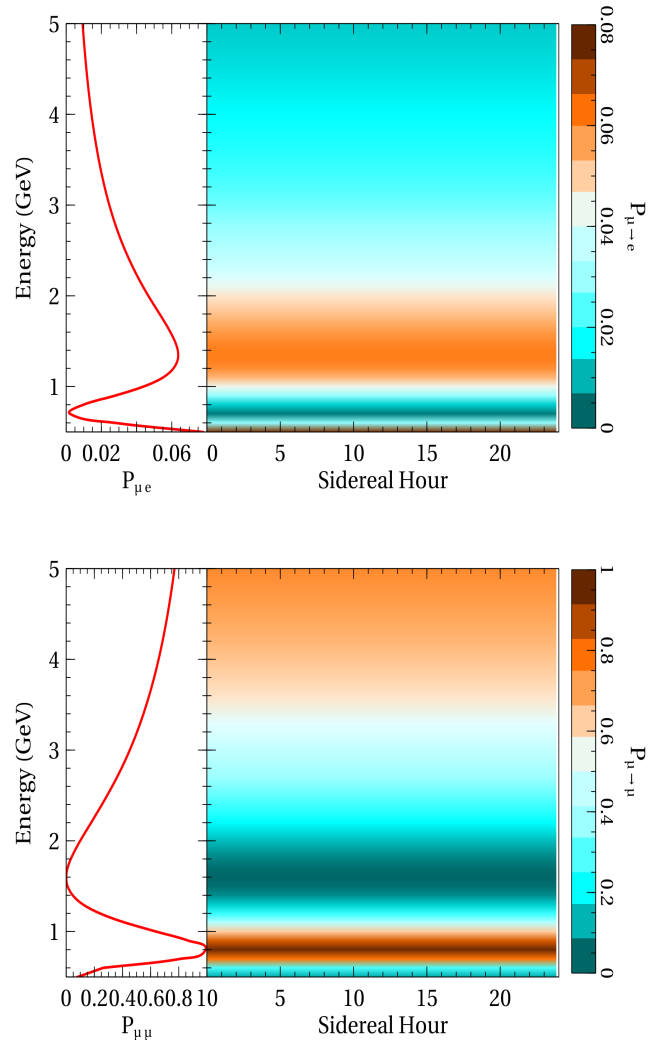


FIG. 1. The standard neutrino oscillation 1-D probability spectrum in terms of energy, as well as the probability distribution in terms of local sidereal time (LST) and energy for the appearance channel (top) and disappearance channel (bottom) without taking LIV parameters into account. The oscillation parameters listed in Table I is adopted to calculate the probability distribution.

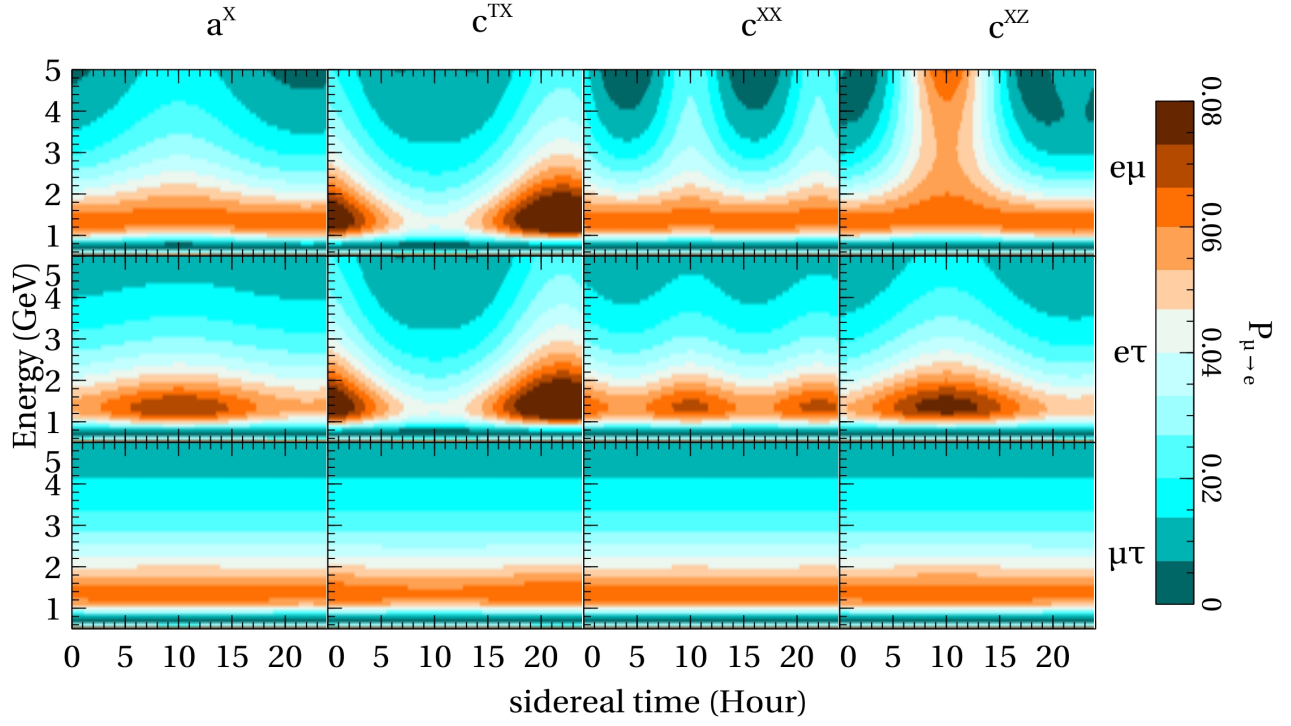


FIG. 2. The probability distribution for the appearance channel is depicted in each panel corresponding to a specific non-zero LIV parameter. In each panel, one specific LIV parameter is set to  $1 \times 10^{-23}$ , while the others are set to 0.

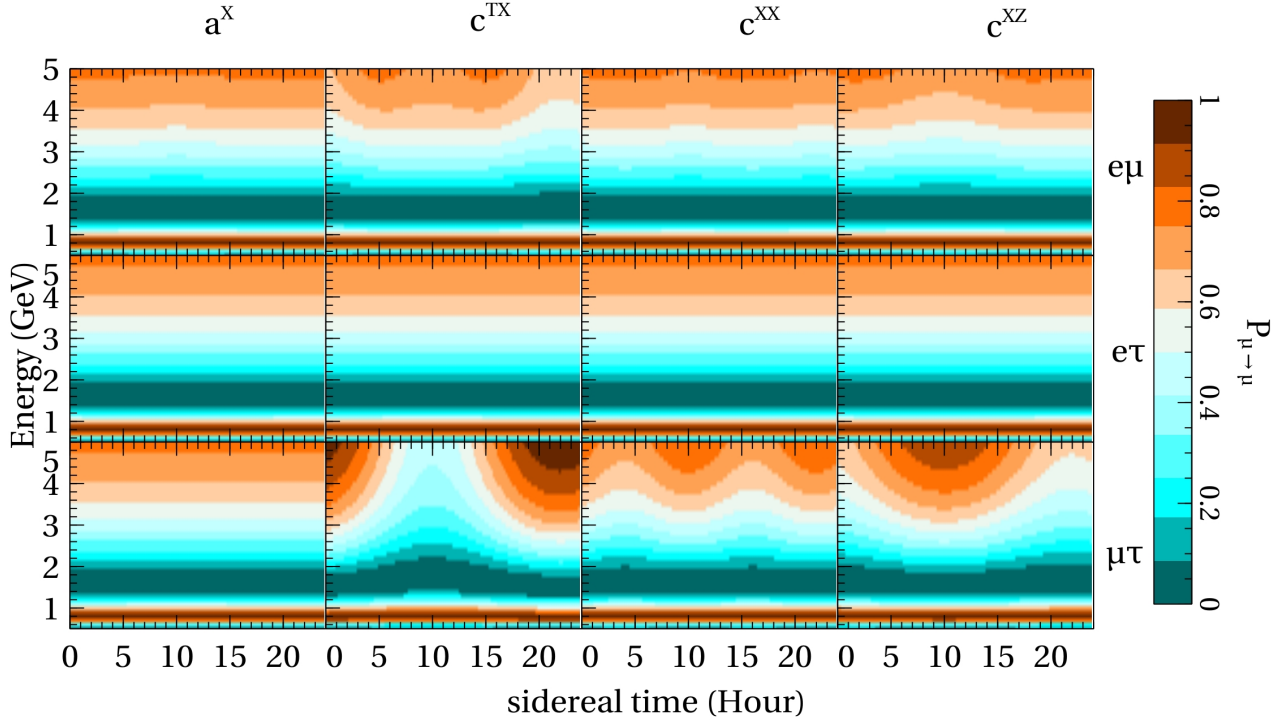


FIG. 3. The probability distribution for the disappearance channel is depicted in each panel corresponding to a specific non-zero LIV parameter. In each panel, one specific LIV parameter is set to  $1 \times 10^{-23}$ , while the others are set to 0.

As we move from left to right in the top panel of Figs. 2 and 3, the probability modulates as  $\omega_{\oplus}$ ,  $\omega_{\oplus}$ ,  $2\omega_{\oplus}$  and  $\omega_{\oplus}$ . This nature is fairly evident for  $e\mu$  and  $e\tau$  coefficients in the appearance channel as well as  $\mu\tau$  coefficients in the disappearance channel, such modulations in data serve as smoking-gun signature for LIV. This particular feature can also be comprehended by referring to Eq. 8, which demonstrates the relative contribution of each parameter and dependency on LST. In the appearance channel, the maximum of oscillation for  $(a)_{e\mu}^X$  and  $(a)_{e\tau}^X$  parameters with respect to energy does not show any observable shift; the only distortion is observed along the sidereal time axis. On the other hand, for  $(c)_{e\mu}^{XX}$  and  $(c)_{e\tau}^{XX}$  parameters shift is strongly correlated with energy. The impact of  $(a)_{\mu\tau}^X$  on appearance probability distribution is minimal. Conversely, the parameters  $(a)_{e\mu}^X$ ,  $(a)_{e\tau}^X$  do not play a significant role in the disappearance channel. This is evident as they do not appear in the leading-order term of the disappearance channel probability.

The primary objectives of all ongoing and prospective high-precision long-baseline neutrino oscillation experiments are to determine the precise CP violating phase ( $\delta_{cp}$ ) and the octant of  $\theta_{23}$ , as well as resolving the mass hierarchy. However, there is significant uncertainties in the current measurement of  $\theta_{23}$  and  $\delta_{cp}$  phase. In the case of long-baseline searches, standard oscillation parameters mix with LIV parameter, introducing a level of uncertainty that can potentially reduce the sensitivity of the experiment to detect the sidereal signal. We therefore investigate the correlations between the LIV parameters and conventional oscillation parameters  $\theta_{23}$  and  $\delta_{cp}$ , while also examining the sensitivity of the NO $\nu$ A experiment to the sidereal effect.

### A. Sensitivity

In order to derive the sensitivity, we adopted the Poisson-likelihood chi-square statistics. The Poisson-likelihood chi-square function for NO $\nu$ A experiment can

be written as: [33]

$$\chi_{total}^2(N_{test}, N_{true}) = \sum_{i,j,k} 2 \left( N_{test}^{ijk} - N_{true}^{ijk} + N_{true}^{ijk} \times \ln \left[ \frac{N_{true}^{ijk}}{N_{test}^{ijk}} \right] \right), \quad (16)$$

where "i" stands for LST bins, "j" for appearance and disappearance channels, and "k" for the beam's neutrino and anti-neutrino modes. The " $N_{true}$ " represents the total number of events in each sidereal bin for energy window of 1 to 5 GeV in the SM case, while " $N_{test}$ " represents the same quantity in the case of LIV. We adopted 24 sidereal bins, each lasting 1 sidereal hour, encompassing the full duration of a sidereal day. The total 5% of systematic uncertainty is considered in final analysis. Systematics is incorporated using so called pull method.

The allowed regions of standard parameters  $\delta_{CP}$  and  $\theta_{23}$  at 95%, 99%, and  $3\sigma$  significance level with respect to LIV parameters  $a_{\alpha\beta}^X$ ,  $c_{\alpha\beta}^{TX}$ ,  $c_{\alpha\beta}^{XX}$ ,  $c_{\alpha\beta}^{XZ}$  are illustrated in Figs 4 and 5, respectively. The LIV parameters of interest possess complex values. The strength of a parameter depends on its phase, therefore, the sensitivity of experiment towards particular LIV parameter is influenced by the phase of that parameter. As the phases of these parameters are unknown, marginalization over full parameter space of LIV phase along with parameter space of  $\delta_{CP}$  and  $\theta_{23}$  is performed. Figure 6 illustrates the variation of sensitivity of NO $\nu$ A to the LIV parameters across the entire range of phase values. We now present the sensitivity of NO $\nu$ A-experiment towards constraining the non-diagonal parameters  $a_{\alpha\beta}^X$ ,  $c_{\alpha\beta}^{TX}$ ,  $c_{\alpha\beta}^{XX}$ ,  $c_{\alpha\beta}^{XZ}$  with  $\alpha \neq \beta$  using the sidereal analysis. With marginalisation over  $\theta_{23}$  and  $\delta_{CP}$ , the degeneracy effect of these parameter is eliminated. Figure 7 illustrates the  $\chi^2$  sensitivity of the LIV parameters in both the appearance and disappearance channels, considering both neutrino and anti-neutrino modes.

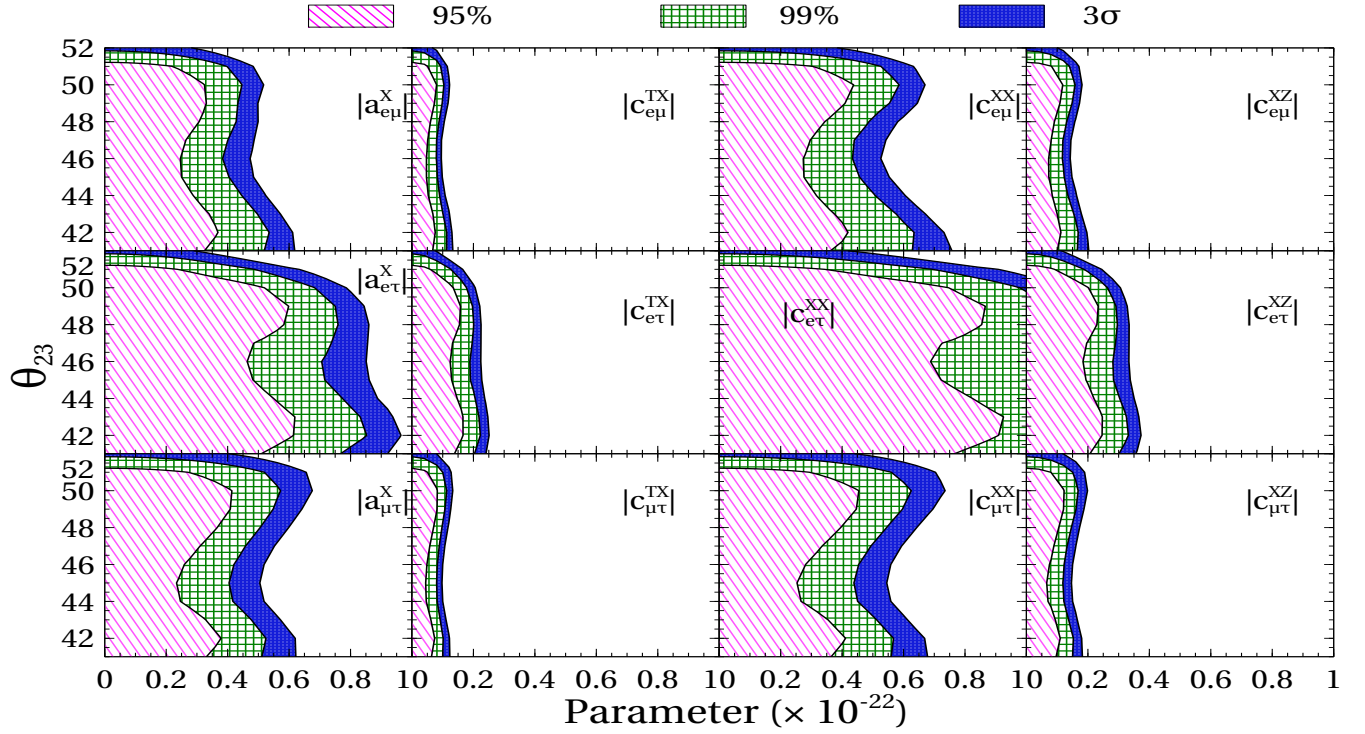


FIG. 4. Correlations between the non-diagonal parameters ( $a_{\alpha\beta}^X$ ,  $c_{\alpha\beta}^{TX}$ ,  $c_{\alpha\beta}^{XX}$ ,  $c_{\alpha\beta}^{XZ}$  with  $\alpha \neq \beta$ ) and mixing angle  $\theta_{23}$  at 95%, 99%, and  $3\sigma$  CL.

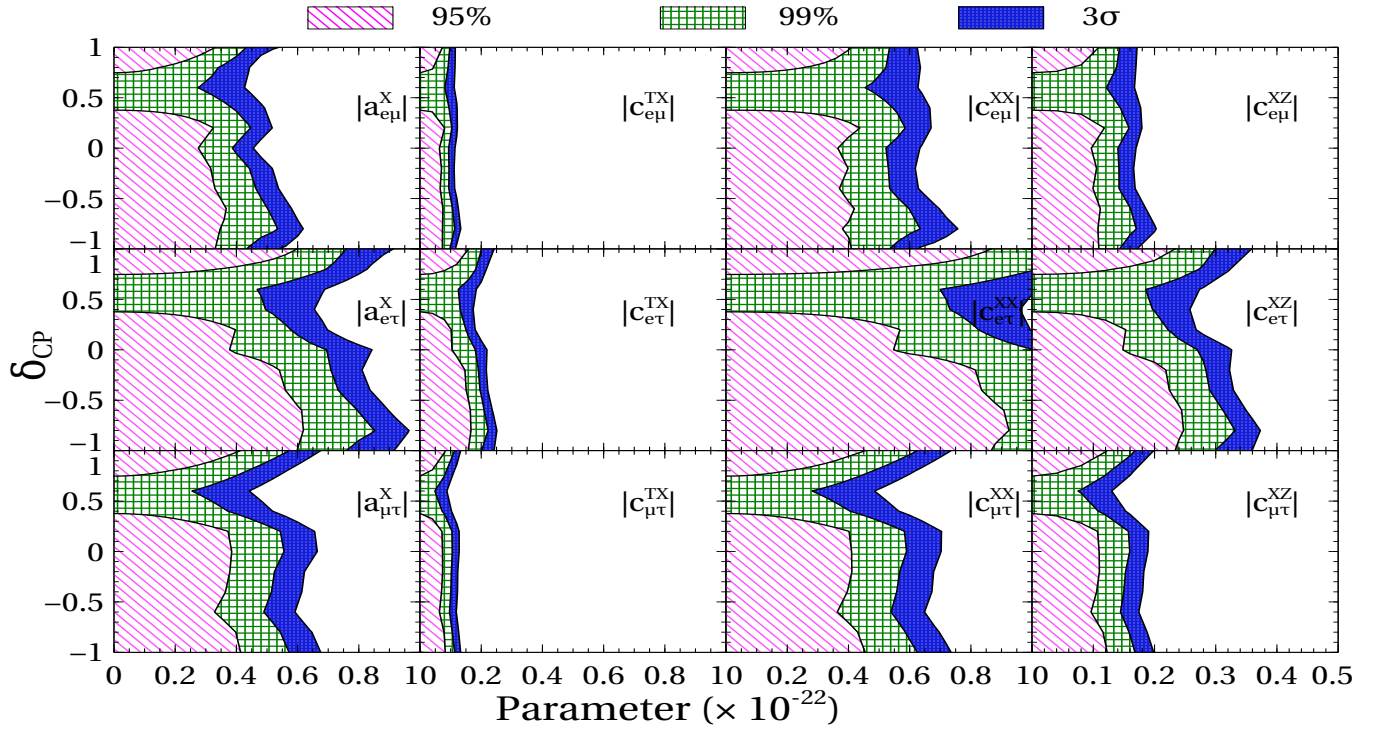


FIG. 5. Correlations between the non-diagonal parameters ( $a_{\alpha\beta}^X$ ,  $c_{\alpha\beta}^{TX}$ ,  $c_{\alpha\beta}^{XX}$ ,  $c_{\alpha\beta}^{XZ}$  with  $\alpha \neq \beta$ ) and Dirac cp-phase  $\delta_{CP}$  at  $2\sigma$ ,  $3\sigma$ , and  $5\sigma$  CL.

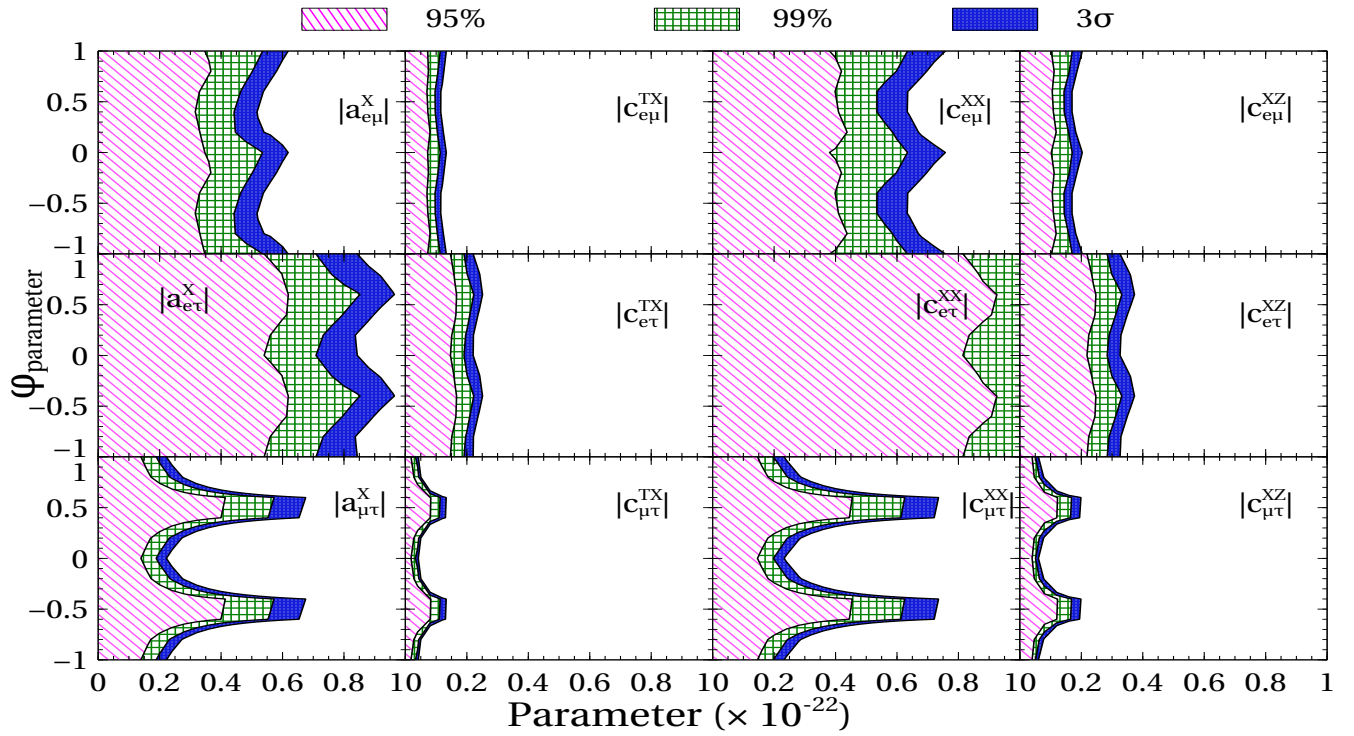


FIG. 6. Correlations between the non-diagonal parameters ( $a_{\alpha\beta}^X$ ,  $c_{\alpha\beta}^{TX}$ ,  $c_{\alpha\beta}^{XX}$ ,  $c_{\alpha\beta}^{XZ}$  with  $\alpha \neq \beta$ ) at  $2\sigma$ ,  $3\sigma$ , and  $5\sigma$  CL

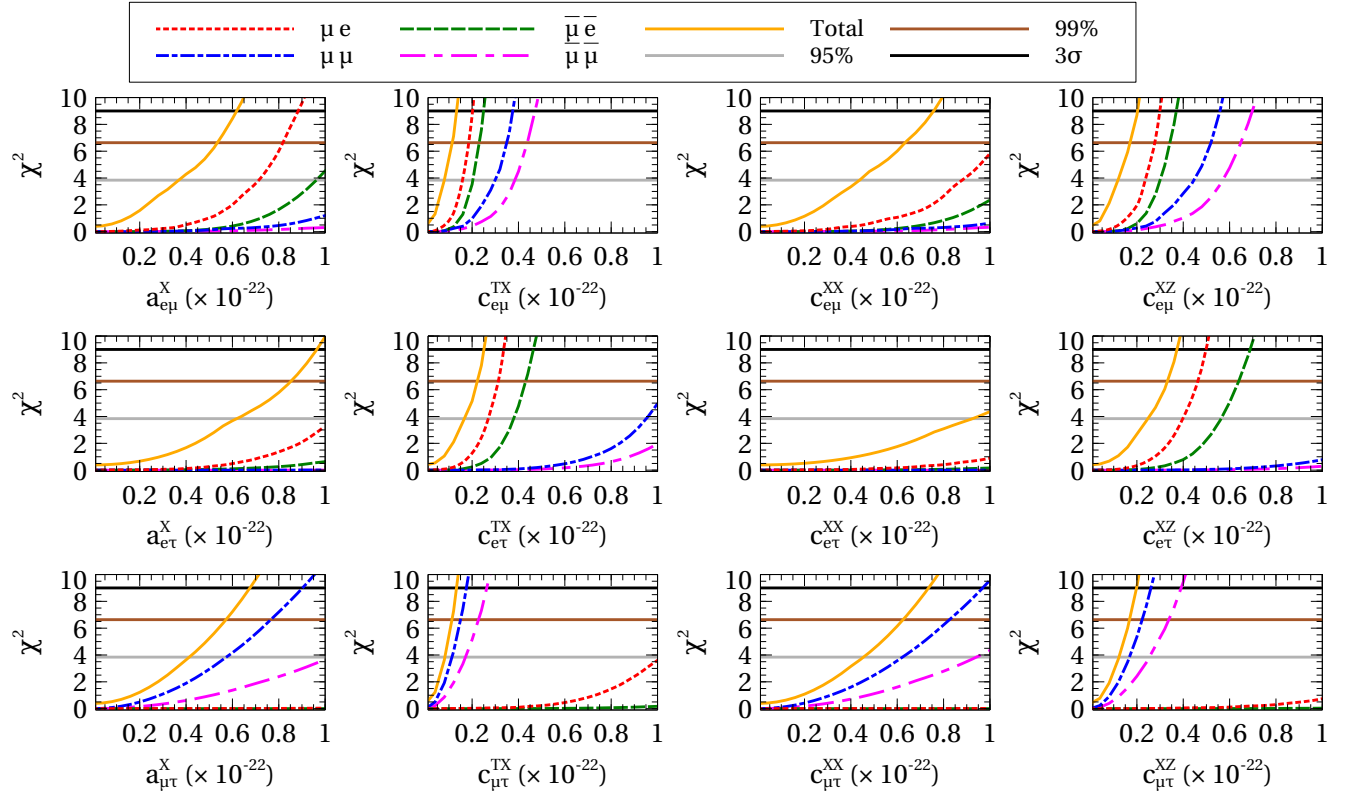


FIG. 7. Sensitivity plots of the LIV parameters for  $\mu e$ ,  $\mu\mu$ ,  $\bar{\mu} e$ ,  $\bar{\mu}\bar{\mu}$  and all channels combined with  $2\sigma$  and  $3\sigma$  cut



TABLE III. Summary of upper limits at 95% and 99.7% C.L. for all 12 LIV parameter under sidereal analysis.

Parameter	Previous limit	References	This work	This work
	$3\sigma$		95% C.L.	99.7% C.L.
$ a_{e\mu}^X  =  a_{e\mu}^Y $	$2.2 \times 10^{-20}$	[12] [14]	$3.68 \times 10^{-23}$	$6.18 \times 10^{-23}$
$ a_{e\tau}^X  =  a_{e\tau}^Y $	NA		$6.2 \times 10^{-23}$	$9.64 \times 10^{-23}$
$ a_{\mu\tau}^X  =  a_{\mu\tau}^Y $	$1.8 \times 10^{-23}$	[15]	$4.13 \times 10^{-23}$	$6.75 \times 10^{-23}$
$ c_{e\mu}^{TX}  =  c_{e\mu}^{TY} $	$9.0 \times 10^{-23}$	[12] [14]	$8.0 \times 10^{-24}$	$1.32 \times 10^{-23}$
$ c_{e\tau}^{TX}  =  c_{e\tau}^{TY} $	NA		$1.66 \times 10^{-23}$	$2.5 \times 10^{-23}$
$ c_{\mu\tau}^{TX}  =  c_{\mu\tau}^{TY} $	$3.7 \times 10^{-27}$	[15]	$8.2 \times 10^{-24}$	$1.32 \times 10^{-23}$
$ c_{e\mu}^{XX}  =  c_{e\mu}^{YY} $	$4.6 \times 10^{-21}$	[12] [14]	$4.38 \times 10^{-23}$	$7.57 \times 10^{-23}$
$ c_{e\tau}^{XX}  =  c_{e\tau}^{YY} $	NA		$9.26 \times 10^{-23}$	--
$ c_{\mu\tau}^{XX}  =  c_{\mu\tau}^{YY} $	$2.5 \times 10^{-23}$	[13]	$4.54 \times 10^{-23}$	$7.35 \times 10^{-23}$
$ c_{e\mu}^{XZ}  =  c_{e\mu}^{YZ} $	$1.1 \times 10^{-21}$	[12] [14]	$1.1 \times 10^{-23}$	$2.04 \times 10^{-23}$
$ c_{e\tau}^{XZ}  =  c_{e\tau}^{YZ} $	NA		$2.46 \times 10^{-23}$	$3.72 \times 10^{-23}$
$ c_{\mu\tau}^{XZ}  =  c_{\mu\tau}^{YZ} $	$0.7 \times 10^{-23}$	[13]	$1.21 \times 10^{-23}$	$1.98 \times 10^{-23}$

By adopting a one-parameter-at-a-time analysis, the upper limits  $3\sigma$  level of all 12 LIV parameters is listed in Table III. We note that sidereal analysis provide more stringent constraints on  $3\sigma$  level for CPT-violating coefficient  $a_{e\mu}^X$  ( $a_{e\mu}^Y$ ) which are suppressed by 3 orders from previous reported results. In this analysis, we present the first time constraint on LIV parameter with subscript  $e\tau$  which have never been reported previously by any neutrino experiment. Only specific channels have been used in previous studies of the sidereal impact in neutrino sectors.  $\text{NO}\nu\text{A}$  is not able to improve the results on  $\mu\tau$  parameters from existing bounds, as the neutrino beam used in  $\text{NO}\nu\text{A}$  is not able to create  $\tau$  hence it is not sensitive for  $\mu \rightarrow \tau$  channel.

## V. SUMMARY AND CONCLUSION

The presented work focuses on investigating Lorentz Invariance Violation (LIV) through the sidereal effect within the context of the  $\text{NO}\nu\text{A}$  experiment. Oscillation probabilities and events are simulated using the GLoBES software with desired experimental configurations. This analysis examines the influence of the sidereal effect on various LIV parameters within the oscillation probability spectra.

As the sidereal effect is time-dependent, the flux variation with sidereal time may alter the event to LST spectra. Since there is no prior experimental data available on flux variation with LST, an average constant flux over the entire sidereal period is considered. It is observed

that Eq. 13 and 14 accurately describe the sidereal effect for the long-baseline scenario. Furthermore, it is demonstrated that LIV parameters exhibit complementary characteristics in the appearance and disappearance channels. Certain parameters predominantly affect the appearance channel, while others primarily impact the disappearance channel. This pattern is also reflected in the sensitivity analysis, as sensitivity is specific to each channel.

By combining the effects from all channels, the  $\text{NO}\nu\text{A}$  experiment can provide new constraints on LIV parameter values at a  $3\sigma$  confidence level. The study indicates that the  $\text{NO}\nu\text{A}$  experiment has the capability to detect and constrain sidereal effects effectively using the far detector. However, not all parameters could be explored with improved limits.

Since non-isotropic LIV is direction-dependent, it cannot be constrained through conventional neutrino oscillation studies. Figs 5 and 4 illustrate that the sidereal effect is sensitive to the standard oscillation parameters  $\theta_{23}$  and  $\delta_{CP}$ . Uncertainties in these parameters can reduce the sensitivity of  $\text{NO}\nu\text{A}$  to sidereal parameters.

Moreover, the sidereal parameters are highly influenced by the baseline length and neutrino energy. Future long-baseline experiments with longer baselines and higher energies, such as DUNE, T2HKK and P2O may offer enhanced sensitivity to non-isotropic LIV parameters.

## VI. ACKNOWLEDGMENTS

We acknowledge financial support from the DST, New Delhi, India for providing funds under the Umbrella

Scheme Research and Development (S. Mishra, S. Shukla, and V. Singh), CSIR, New Delhi, India (S. Shukla) and UGC-BSR Research Start Up Grant, India Contract F.30-584/2021 (BSR) (L. S.). We would like to thank Dr. M. Masud for many insightful discussions.

- 
- [1] V. A. Kostelecky and S. Samuel, Spontaneous Breaking of Lorentz Symmetry in String Theory, *Phys. Rev. D* **39**, 683 (1989).
- [2] V. A. Kostelecky and R. Potting, CPT and strings, *Nucl. Phys. B* **359**, 545 (1991).
- [3] R. Gambini and J. Pullin, Nonstandard optics from quantum space-time, *Phys. Rev. D* **59**, 124021 (1999), [arXiv:gr-qc/9809038](#).
- [4] C. P. Burgess, J. M. Cline, E. Filotas, J. Matias, and G. D. Moore, Loop-generated bounds on changes to the graviton dispersion relation, *Journal of High Energy Physics* **2002**, 043 (2002).
- [5] S. Sahoo, A. Kumar, and S. K. Agarwalla, Probing Lorentz Invariance Violation with atmospheric neutrinos at INO-ICAL, *JHEP* **03**, 050, [arXiv:2110.13207 \[hep-ph\]](#).
- [6] D. Colladay and V. A. Kostelecky, Lorentz violating extension of the standard model, *Phys. Rev. D* **58**, 116002 (1998), [arXiv:hep-ph/9809521](#).
- [7] R. Bluhm, Overview of the SME: Implications and phenomenology of Lorentz violation, *Lect. Notes Phys.* **702**, 191 (2006), [arXiv:hep-ph/0506054](#).
- [8] V. A. Kostelecký and N. Russell, Data tables for lorentz and *cpt* violation, *Rev. Mod. Phys.* **83**, 11 (2011).
- [9] Y. Fukuda *et al.* (Super-Kamiokande), Measurements of the solar neutrino flux from Super-Kamiokande's first 300 days, *Phys. Rev. Lett.* **81**, 1158 (1998), [Erratum: *Phys.Rev.Lett.* **81**, 4279 (1998)], [arXiv:hep-ex/9805021](#).
- [10] K. Eguchi *et al.* (KamLAND), First results from KamLAND: Evidence for reactor anti-neutrino disappearance, *Phys. Rev. Lett.* **90**, 021802 (2003), [arXiv:hep-ex/0212021](#).
- [11] M. H. Ahn *et al.* (K2K), Measurement of Neutrino Oscillation by the K2K Experiment, *Phys. Rev. D* **74**, 072003 (2006), [arXiv:hep-ex/0606032](#).
- [12] P. Adamson *et al.* (MINOS), Testing Lorentz Invariance and CPT Conservation with NuMI Neutrinos in the MINOS Near Detector, *Phys. Rev. Lett.* **101**, 151601 (2008), [arXiv:0806.4945 \[hep-ex\]](#).
- [13] P. Adamson *et al.* (MINOS), A Search for Lorentz Invariance and CPT Violation with the MINOS Far Detector, *Phys. Rev. Lett.* **105**, 151601 (2010), [arXiv:1007.2791 \[hep-ex\]](#).
- [14] P. Adamson *et al.* (MINOS), Search for Lorentz invariance and CPT violation with muon antineutrinos in the MINOS Near Detector, *Phys. Rev. D* **85**, 031101 (2012), [arXiv:1201.2631 \[hep-ex\]](#).
- [15] R. Abbasi *et al.* (IceCube), Search for a Lorentz-violating sidereal signal with atmospheric neutrinos in IceCube, *Phys. Rev. D* **82**, 112003 (2010), [arXiv:1010.4096 \[astro-ph.HE\]](#).
- [16] L. B. Auerbach *et al.* (LSND), Tests of Lorentz violation in anti- $\nu(\mu) \rightarrow$  anti- $\nu(e)$  oscillations, *Phys. Rev. D* **72**, 076004 (2005), [arXiv:hep-ex/0506067](#).
- [17] K. Abe *et al.* (Super-Kamiokande), Test of Lorentz invariance with atmospheric neutrinos, *Phys. Rev. D* **91**, 052003 (2015), [arXiv:1410.4267 \[hep-ex\]](#).
- [18] K. Abe *et al.* (T2K), Search for Lorentz and CPT violation using sidereal time dependence of neutrino flavor transitions over a short baseline, *Phys. Rev. D* **95**, 111101 (2017), [arXiv:1703.01361 \[hep-ex\]](#).
- [19] D. Adey *et al.* (Daya Bay), Search for a time-varying electron antineutrino signal at Daya Bay, *Phys. Rev. D* **98**, 092013 (2018), [arXiv:1809.04660 \[hep-ex\]](#).
- [20] A. A. Aguilar-Arevalo *et al.* (MiniBooNE), Test of Lorentz and CPT violation with Short Baseline Neutrino Oscillation Excesses, *Phys. Lett. B* **718**, 1303 (2013), [arXiv:1109.3480 \[hep-ex\]](#).
- [21] Y. Abe *et al.* (Double Chooz), First Test of Lorentz Violation with a Reactor-based Antineutrino Experiment, *Phys. Rev. D* **86**, 112009 (2012), [arXiv:1209.5810 \[hep-ex\]](#).
- [22] G. Barenboim, M. Masud, C. A. Ternes, and M. Tórtola, Exploring the intrinsic Lorentz-violating parameters at DUNE, *Phys. Lett. B* **788**, 308 (2019), [arXiv:1805.11094 \[hep-ph\]](#).
- [23] M. A. Acero *et al.* (NOvA), First Measurement of Neutrino Oscillation Parameters using Neutrinos and Antineutrinos by NOvA, *Phys. Rev. Lett.* **123**, 151803 (2019), [arXiv:1906.04907 \[hep-ex\]](#).
- [24] J. S. Diaz, V. A. Kostelecky, and M. Mewes, Perturbative Lorentz and CPT violation for neutrino and antineutrino oscillations, *Phys. Rev. D* **80**, 076007 (2009), [arXiv:0908.1401 \[hep-ph\]](#).
- [25] J. Kopp, M. Lindner, T. Ota, and J. Sato, Non-standard neutrino interactions in reactor and superbeam experiments, *Phys. Rev. D* **77**, 013007 (2008), [arXiv:0708.0152 \[hep-ph\]](#).
- [26] V. A. Kostelecky and M. Mewes, Lorentz and CPT violation in the neutrino sector, *Phys. Rev. D* **70**, 031902 (2004), [arXiv:hep-ph/0308300](#).
- [27] V. A. Kostelecky and M. Mewes, Lorentz violation and short-baseline neutrino experiments, *Phys. Rev. D* **70**, 076002 (2004), [arXiv:hep-ph/0406255](#).
- [28] D. S. Ayres *et al.* (NOvA), The NOvA Technical Design Report, FERMILAB-DESIGN-2007-01 [10.2172/935497](#) (2007).
- [29] P. Huber, M. Lindner, and W. Winter, Simulation of long-baseline neutrino oscillation experiments with GLOBES (General Long Baseline Experiment Simulator), *Comput. Phys. Commun.* **167**, 195 (2005), [arXiv:hep-ph/0407333](#).
- [30] P. Huber, J. Kopp, M. Lindner, M. Rolinec, and W. Winter, New features in the simulation of neutrino oscillation experiments with GLOBES 3.0: General Long Baseline Experiment Simulator, *Comput. Phys. Commun.* **177**, 432 (2007), [arXiv:hep-ph/0701187](#).

- [31] P. B. Denton and J. Gehrlein, Here comes the sun: Solar parameters in long-baseline accelerator neutrino oscillations (2023), [arXiv:2302.08513 \[hep-ph\]](#).
- [32] I. Esteban, M. C. Gonzalez-Garcia, M. Maltoni, T. Schwetz, and A. Zhou, The fate of hints: updated global analysis of three-flavor neutrino oscillations, *JHEP* **09**, 178, [arXiv:2007.14792 \[hep-ph\]](#).
- [33] S. Baker and R. D. Cousins, Clarification of the Use of Chi Square and Likelihood Functions in Fits to Histograms, *Nucl. Instrum. Meth.* **221**, 437 (1984).
- [34] J. Liao, D. Marfatia, and K. Whisnant, Degeneracies in long-baseline neutrino experiments from non-standard interactions, *Phys. Rev.* **D93**, 093016 (2016), [arXiv:1601.00927 \[hep-ph\]](#).
- [35] M. Esteves Chaves, D. Rossi Gratieri, and O. L. G. Peres, Improvements on perturbative oscillation formulas including non-standard neutrino Interactions, (2018), [arXiv:1810.04979 \[hep-ph\]](#).
- [36] U. K. Dey, N. Nath, and S. Sadhukhan, Non-Standard Neutrino Interactions in a Modified  $\nu$ 2HDM, *Phys. Rev.* **D98**, 055004 (2018), [arXiv:1804.05808 \[hep-ph\]](#).
- [37] O. Yasuda, On the exact formula for neutrino oscillation probability by Kimura, Takamura and Yokomakura, (2007), [arXiv:0704.1531 \[hep-ph\]](#).
- [38] M. Masud, A. Chatterjee, and P. Mehta, Probing CP violation signal at DUNE in presence of non-standard neutrino interactions, *J. Phys.* **G43**, 095005 (2016), [arXiv:1510.08261 \[hep-ph\]](#).
- [39] M. Masud and P. Mehta, Nonstandard interactions spoiling the CP violation sensitivity at DUNE and other long baseline experiments, *Phys. Rev.* **D94**, 013014 (2016), [arXiv:1603.01380 \[hep-ph\]](#).
- [40] M. Masud and P. Mehta, Nonstandard interactions and resolving the ordering of neutrino masses at DUNE and other long baseline experiments, *Phys. Rev.* **D94**, 053007 (2016), [arXiv:1606.05662 \[hep-ph\]](#).
- [41] R. Majhi, S. Chembra, and R. Mohanta, Exploring the effect of Lorentz invariance violation with the currently running long-baseline experiments, *Eur. Phys. J. C* **80**, 364 (2020), [arXiv:1907.09145 \[hep-ph\]](#).
- [42] A. Chatterjee, F. Kamiya, C. A. Moura, and J. Yu, Impact of Matter Density Profile Shape on Non-Standard Interactions at DUNE, (2018), [arXiv:1809.09313 \[hep-ph\]](#).